Theor Chem Acc (1997) 97:313–316

Theoretical
Chemistry Accounts

The unimolecular chemistry of protonated glycine and the proton affinity of glycine: a computational model

Einar Uggerud

Department of Chemistry, University of Oslo, P.O. Box 1033 Blindern, N-0315 Oslo, Norway

Received: 15 November 1996 / Accepted: 6 May 1997

Abstract. The potential energy hypersurface of protonated glycine, GH^+, has been investigated. The calculated G2(MP2) value for the proton affinity (PA) of glycine, $PA_{calc} = 895\,kJ\ mol^{-1}$, is in good agreement with the experimental value which has been estimated to lie in the range $864\,kJ\ mol^{-1} < PA_{exp} < 891\,kJ\ mol^{-1}$. Ab initio quantum chemical calculations of relevant parts of the potential energy surface of GH^+ give a reaction model which is consistent with the observed mass spectrometric fragmentation pattern. The lowest energy unimolecular reactions of GH^+ are two distinct processes: (1) loss of CO, which has a substantial barrier for the reverse reaction, and (2) loss of CO plus H_2O, which has no barrier for the reverse reaction.

Key words: Protonated glycine – Proton affinity – Unimolecular reactions – Mass spectrometry – Ab inito

1 Introduction

The chemistry of protonated amino acids and peptides is attracting much attention at present [1, 2]. Protonated peptides are routinely formed by a great variety of ionization methods including fast atom bombardment [3] laser desorption [4], electrospray [5], chemical ionization [6] and plasma desorption [7]. Determination of the mass-to-charge ratio (m/z) of the MH^+ ions so formed gives important molecular weight information. In addition to this a lot of information about the structure of peptides can be gained by consideration of their mass spectral fragmentation patterns. Both the identity of the amino acids that constitute the peptide and their sequence can be determined in this way.

Of special interest in this connection is the mechanism by which protonated peptides cleave. The complexity of these macromolecules poses a significant impediment to any detailed evaluation of the energetics or mechanisms of the reactions which generate the mass spectrum.

A peptide has a number of basic sites which can be protonated [8]. The fragmentation pattern is determined by a number of factors. These factors are the kinetics and energetics of the initial proton transfer reaction and the subsequent (usually heterolytic) bond-breaking reactions. The availability (in both the thermodynamic and the kinetic sense) of the different basic sites as well as the lability towards homolytic cleavage of the bonds that are protonated are known to be important factors [9, 10]. Rearrangements prior to bond cleavage of molecular groups via electrostatically bonded ion/molecule complexes [11–14] within the protonated peptide should be considered to be significant.

We have recently conducted a combined experimental and theoretical study of the unimolecular chemistry of protonated formamide [15]. Formamide is the simplest molecule that contains a peptide bond. The activation energies and mechanisms for the three unimolecular reactions observed, (1) loss of water, (2) loss of ammonia, and (3) loss of carbon monoxide, were determined. We then conducted a study of the slightly more complex system, namely protonated glycinamide, GH^+ [16]. Two major unimolecular processes were found, namely (1) loss of ammonia and (2) loss of ammonia plus carbon monoxide. As the next step in our project we are now able to present the results of a computational study of protonated glycine.

2 Theoretical methods

The program system GAUSSIAN 94 [17] was used for the calculations. The molecular geometries of all species relevant to the unimolecular chemistry of protonated glycinamide were first optimized using the 3-21G basis set [18] at the Hartree Fock (HF) level of theory [19]. Start geometries for the transition structure optimizations were obtained by the linear synchronous transit method [20] or by crude interpolation of reactant and product geometries. A combination of the Newton algorithm and normal co-ordinate following algorithms were used for the all geometry optimizations. Starting from each of the optimized transition structure geometries, the intrinsic reaction co-ordinate [21] paths were calculated to ensure the correspondence between the transition structure and the reactant and the product

structures. The optimized geometries were checked for the correct number of negative eigenvalues of the Hessian (the second derivative matrix). The HF/3-21G geometries were used as the start geometries for the final stage of the optimizations. At this stage the wave functions were calculated using the Möller Plesset perturbation theory to the second order [22] and with a 6-31G(*d*,*p*) basis set [23]. Analytical force constants were computed at this stage and the vibrational frequencies were obtained. These vibrational frequencies were used for the final zero point vibrational energy correction after scaling by a factor of 0.94 [24]. The optimized MP2/6-31G(*d*,*p*) geometries and energies together with the corresponding zero point energies provide the final results. To obtain the highest level theoretical estimate of the proton affinity G2(MP2) [25, 26] calculations were in addition performed for glycine and the most stable isomer of protonated glycine.

3 The proton affinity of glycine

The proton affinity (*PA*) of glycine has been determined experimentally by a number of workers over the years. Depending on the method used the *PA* has been estimated to lie in the range $PA = 864 - 891\ \mathrm{kJ\ mol^{-1}}$ [27–30].

Previous theoretical calculations of the isomers of protonated glycine and the proton affinity of glycine have been published by Bouchonnet and Hoppilliard [31] and by Jensen [32]. Bouchonnet and Hoppilliard performed their calculations with MP2/6-31G(*d*)//3-21G and Jensen with MP2/6-31G(*d*)//HF/6-31G(*d*). The two studies agree in that by far the most basic site is the amino group and they calculate the absolute proton affinity to be $PA = 935\ \mathrm{kJ\ mol^{-1}}$ and $PA = 932\ \mathrm{kJ\ mol^{-1}}$, respectively. Our study differs from these two in that we have conducted the geometry optimizations with a larger basis set and included electron correlation in the form of Møller Plesset theory (MP2).

The significance of this methodical difference is reflected in the results. A number of the structures found to be potential energy minima with HF/6-31G(*d*) are not stable with MP2/6-31G(*d*,*p*). This applies to a number of conformers of the carbonyl protonated form (**3**) and the hydroxyl protonated form (**4**) which involves hydrogen bonding to the amino group. The only stable forms found with MP2/6-31G(*d*,*p*) are structures **2**–**4** depicted in Fig. 1. The other HF/6-31G(*d*) minima collapse to the amino protonated form (**2**) upon complete geometry optimization with MP2/6-31G(*d*,*p*). Our energy data are summarized in Table 1. Isomer (**2**) was calculated (with MP2/6-31G(*d*,*p*)) to be $124\ \mathrm{kJ\ mol^{-1}}$ more stable than the carbonyl protonated form (**3**), which in turn is $17\ \mathrm{kJ\ mol^{-1}}$ more stable than the hydroxyl protonated isomer (**4**). The two latter isomers correspond to very shallow minima, and it should be noted that they easily isomerize to (**2**) upon simple rotation around one or two of the single bonds.

With MP2/6-31G(*d*,*p*) we obtain an absolute proton affinity of $PA_{\mathrm{calc}} = 925\ \mathrm{kJ\ mol^{-1}}$ based on the most stable isomer (**2**). Absolute *PA*s obtained at this level of theory are known to be systematically overestimated [33, 34]. When we instead compare the calculated proton affinity of glycine with that of ammonia we find the former to be $25\ \mathrm{kJ\ mol^{-1}}$ higher. By comparison with the known experimental *PA* of ammonia we estimate the theoretical proton affinity glycinamide to be $PA_{\mathrm{calc}} = 888\ \mathrm{kJ\ mol^{-1}}$, which is in satisfactory agreement with the experimental values.

It has been demonstrated that post-Hartree-Fock calculation with large basis sets generally gives absolute theoretical *PA*s that are correct within $10-20\ \mathrm{kJ\ mol^{-1}}$ [26]. One method that has this potential is G2(MP2), so the energies of G (**1**) and GH^+ (**2**) were calculated using this method. The absolute proton affinity obtained, $PA_{\mathrm{calc}} = 895\ \mathrm{kJ\ mol^{-1}}$, compares rather well with the experimental estimates which lie in the range $PA_{\mathrm{exp}} = 864 - 891\ \mathrm{kJ\ mol^{-1}}$.

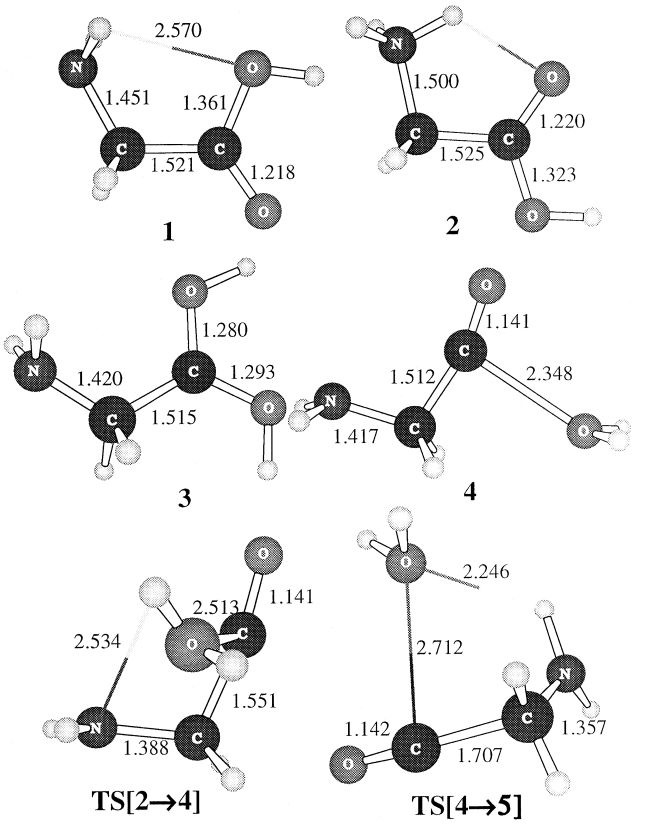

Fig. 1. Molecular structures (MP2/6-31G(*d*,*p*)) of glycine (**1**), its three isomeric protonated forms (**2**)–(**4**) and the found transition structures. Bond distances are given in angstroms

4 Unimolecular fragmentation

Beranová et al. [35] studied the unimolecular decomposition of protonated glycine by various tandem mass spectrometry methods. The lowest energy pathways were inferred by inspection of the metastable ion (MI) decomposition pattern:

Table 1. Results from ab initio calculations

[a] Molecular potential energy obtained from geometry optimized MP2(FC)/6-31G(*d,p*) structures, not including zero point vibrational energies
[b] These numbers give PA (glycine) = 895 kJ mol^{-1}
[c] Zero point vibrational energies. Vibrational frequencies were calculated at MP2/6-31G(*d,p*) optimized structures and are scaled by a factor of 0.94

Molecule	Energy[a] (MP2/6-31G(*d,p*)) [Hartree]	Enthalpy[b] (G2/MP2) [Hartree]	E(z.p.v.)[c] [kJ mol^{-1}]
NH_2CH_2COOH (**1**)	−283.64420	−284.00059	202
$NH_3^+CH_2COOH$ (**2**)	−284.00774	−284.33893	238
$NH_2CH_2COH^+OH$ (**3**)	−283.95852	–	233
$NH_2CH_2COOH_2^+$ (**4**)	−283.94647	–	218
$OC\cdots CH_2NH_2^+\cdots OH_2$ (**5**)	−283.97704	–	214
$CH_2NH_2^+\cdots OH_2$ (**6**)	−170.94896	–	199
$CH_2NH_2^+$ (**7**)	−94.69164	–	138
H_2O (**8**)	−76.21979	–	54
CO (**9**)	−113.02122	–	12
$OC\cdots CH_2NH_2^+$ (**10**)	−207.72158		154
TS[**2** → **4**]	−283.94365	–	217
TS[**4** → **5**]	−283.94423	–	218

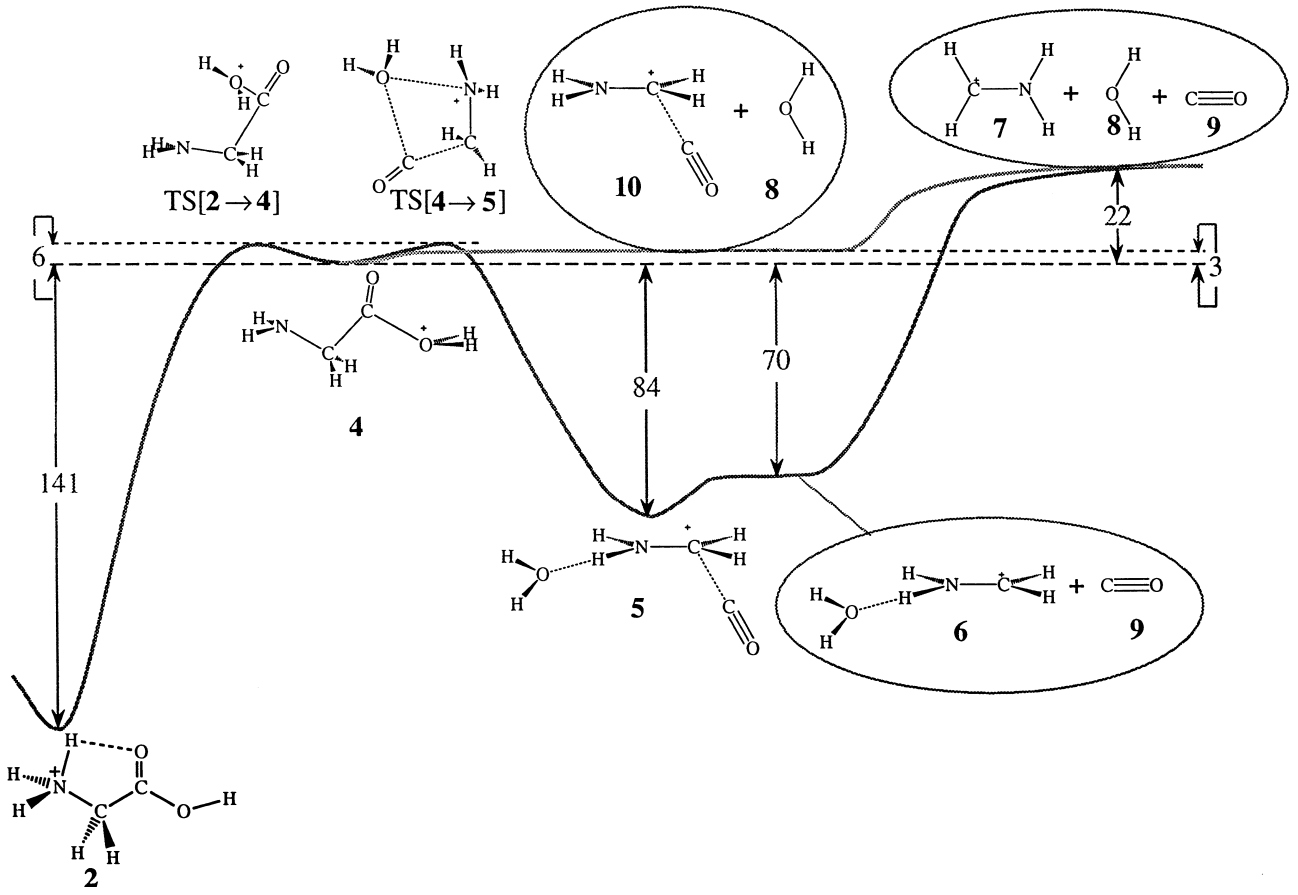

Fig. 2. Potential energy profile for unimolecular decomposition of protonated glycine (GH^+) obtained from the ab initio calculations (energy data of Table 1)

$$[NH_2CH_2COOH]H^+ \rightarrow [NH_2CH_2, H_2O]^+ + CO \quad (1)$$

$$[NH_2CH_2COOH]H^+ \rightarrow [NH_2CH_2]^+ + CO + H_2O \quad (2)$$

Loss of carbon monoxide, reaction (1), dominates the MI spectrum and gives a broad peak in the energy spectrum which corresponds to a substantial translational energy release of $T_{0.5} = 44\,\text{kJ mol}^{-1}$. Reaction (2) is characterized by a much narrower peak, corresponding to a negligible translational energy release.

The part of the potential energy hypersurface of GH^+ which is relevant to the unimolecular chemistry was calculated at the MP2/6-31G(*d,p*) level of theory. The energy data were corrected for differences in zero-point vibrational energies and are reproduced in Table 1 and Fig. 2.

Starting from the most stable isomer of GH^+ (the amino protonated form, **2**) loss of CO is shown to proceed in two steps. In the first step a proton is transferred to the carboxylic acid site and the isomer (**4**) is formed as an intermediate. The key to the CO loss reaction is the transition structure TS[**4** → **5**]. The geometry of TS[**4** → **5**] is shown in Fig. 1 and involves

rearrangement of the hydroxyl OH_2 group. The energy of this transition structure is 172 kJ mol^{-1} above (**2**). Upon rearrangement via TS[**4** → **5**] the isomer (**5**) is formed as a transient intermediate. From this isomer CO is lost immediately owing to the almost vanishingly low C···C bond dissociation energy. The product ion has the structure $CH_2NH_2^+ \cdots OH_2$ (**6**), as determined by calculation of the intrinsic reaction coordinate pathway. This rearrangement followed by fragmentation is seen to give rise to a substantial barrier for the reverse reaction (76 kJ mol^{-1}). This is in agreement with the experimental observation that the reaction is accompanied by a significant translation energy release of $T_{0.5} = 44$ kJ mol^{-1} (which corresponds to 58% of the calculated reverse barrier).

The fate of the $CH_2NH_2^+ \cdots OH_2$ (**6**) ion depends on the internal energy of the GH^+ ions. If the internal energy is sufficiently high, water may be lost in a second step. The products $CH_2NH_2^+ + CO + H_2O$ are only 16 kJ mol^{-1} above TS[**4** → **5**], so energy rich GH^+ ions could have given rise to these products. For metastable ions [35] which only have a few kJ mol^{-1} in addition to TS[**4** → **5**], the situation is different. During CO loss a sufficiently large proportion of the internal energy of the GH^+ ion is given away to relative translation, and therefore these ions will end up as unreactive $[CH_2NH_2^+ \cdots OH_2]^+$ ions.

An alternative and more likely mechanism for loss of the elements of CO and H_2O must therefore exist for long-lived metastable GH^+ ions, which decompose during flight through the analyser tube of the mass spectrometer. Starting from isomer (**4**), direct scission of the C—O bond will give $[H_2NCH_2 \cdots CO]^+$(**10**) + H_2O (**8**). The absence of the intermediate **10** in the MI spectrum [35] is in good accordance with the finding that this is a very weakly bonded complex. Loss of CO will therefore most likely occur directly upon H_2O loss. Separate calculations show that the lengthening of the C—O bond which precedes H_2O loss leads to a simultaneous weakening of the bond between $[NH_2CH_2]^+$ and CO. The best description of the process is therefore that H_2O and CO are lost simultaneously, but via an asynchronous mechanism, where lengthening of the C···O bond precedes lengthening of the C···C bond. The reaction has no transition structure and is classified as a type I reaction, having a loose transition state. According to the MP2 calculations the potential energy of the products, $[NH_2CH_2]^+ + CO + H_2O$, is 16 kJ mol^{-1} higher than TS[**4** → **5**]. This is in good agreement with the experimental data, which shows that loss of CO dominates over loss of CO plus H_2O.

In conclusion a unimolecular reaction model, which is consistent with available experimental data, has been presented.

Acknowledgemets. E.U. wishes to thank the Norwegian Research Council (NFR) and VISTA for the grants which made this work possible. The calculations were made possible thanks to support through the NFR Programme for Supercomputing.

References

1. Desiderio DM (ed) (1991) Mass Spectrometry of Peptides; CRC Press, Boca Raton
2. McEwen C, Larsen B, (eds) (1991) Mass Spectrometry of Biological Materials; Marcel Dekker, New York
3. Barber M, Bordioli RS, Sedwick RD, Tyler AN (1981) J Chem Soc Chem Commun p 325
4. Karas M, Hillenkamp (1988) F Anal Chem 60:2299
5. Wong SF, Meng, CK, Fenn JB (1988) J Phys Chem 92:546
6. Harrison AG (1992) Chemical Ionization Mass Spectrometry, 2nd edn. CRC, Boca Raton
7. Jonsson GP, Hedin AB, Häkansson PL, Sundquist BU, Save GBS, Nielsen PF, Roepstorff P, Johansson K-E, Kamensky I, Lindberg MSL (1986) Anal Chem 58:1084
8. Yeh RW, Grimley JM, Bursey MM (1991) Biol Mass Spectrom 20:443
9. Nakata H, Suzuki K-I, Takeda N, Tatematsu A (1988) Org Mass Spectrom 16:188
10. Nakata H, Kadoguchi K, Konishi H, Takeda N, Tatematsu A (1993) Org Mass Spectrom 28:67
11. Bowen RD, Stapleton J, Williams DH (1978) Tetrahedron Lett 2919
12. Bowen RD, Williams DH, Schwarz H, Wesdemiotis C (1979) J Chem Soc, Chem Commun p 261
13. Longvialle P, Botter R (1980) J Chem Soc, Chem Commun 823
14. Morton TH (1983) Tetrahedron, 38:3195
15. Lin HY, Ridge DP, Vulpius T, Uggerund E (1994) J Am Chem Soc 116:2996
16. Kinser RD, Ridge DP, Hvistendahl G, Rasmussen B, Uggerud E (1996) Chemistry – A European Journal 2:1143
17. Frisch MJ, Trucks GW, Schlegel HB, Gill PMW, Johnson BG, Robb MA, Cheeseman JR, Keith TA, Peterson GA, Mongomery JA, Raghavachari K, Al-Laham MA, Zakrzewski VG, Ortiz JV, Foresman JB, Cioslowski J, Stefanov BB, Nanayakkara A, Challacombe M, Peng CY, Ayala PY, Chen W, Wong MW, Andres JL, Reploge ES, Gomperts R, Martin RL, Fox DJ, Binkley JS, Defrees DJ, Baker J, Stewart JJP, Head-Gordon M, Gonzalez C, Pople JA (1994) Gaussian Inc, Pittsburgh, Pa
18. Hehre WJ, Ditchfield R, Pople JA (1972) J Am Chem Soc 56:2257
19. Roothan CCJ (1951) Rev. Mod. Phys 23:69
20. Halgren TA, Lipscomb WM (1977) Chem Phys Lett 49:225
21. Gonzales C, Schlegel HB (1989) J Phys Chem 90:2154
22. Möller C, Plesset MS (1934) Phys Rev 46:618
23. Frisch MJ, Pople JA, Binkley JS (1984) J Chem Phys 80:3265
24. Pople JA, Scott AP, Wong MW, Radom L (1993) Israel J Chem 33:345
25. Curtiss LA, Raghavachari K, Pople JA (1993) J Chem Phys 98:1293
26. Smith BJ, Radom L (1994) Chem Phys Lett p 231
27. Gorman GS, Speir JP, Turner CA, Amster IJ (1992) J Am Chem Soc 114:3986
28. Wu J, Lebrilla CB (1993) J Am Chem Soc 115:3270
29. Locke MJ, Hunter RL, McIver RT (1979) J Am Chem Soc 101:272
30. Meot-Ner M, Hunter EP, Field F (1979) J Am Chem Soc 101:686
31. Bouchonnet S, Hoppilliard Y (1992) Org Mass Spectrom 27:71
32. Jensen F (1992) J Am Chem Soc 114:9533
33. Dixon DA, Lias SG (1987) In: Liebman JL, Greenberg A (eds) Molecular structure and energetics, vol. 2: physical measurements. VCH, New York, pp 269
34. Uggerud E (1992) Mass Spectrom Rev 11 389
35. Beranová S, Cai J, Wesdemiotis C (1995) J Am Chem Soc 117:9492